

Supplementary Material For

Ability of Density Functional Theory Methods to

Accurately Model the Reaction Energy Pathways

of the Oxidation of CO on Gold Cluster: A

Benchmark Study

Saumya Gurtu,[†] Sandhya Rai,[†] Masahiro Ehara,[‡] and U. Deva Priyakumar^{*,†}

Center for Computational Natural Sciences and Bioinformatics, International Institute of Information Technology, Hyderabad, India, and Research Center for Computational Science, Institute for Molecular Science, 38 Nishigo-Naka, Myodaiji, Okazaki 444-8585, Japan

E-mail: deva@iiit.ac.in

^{*}To whom correspondence should be addressed

[†]Center for Computational Natural Sciences and Bioinformatics, International Institute of Information Technology, Hyderabad, India

[‡]Research Center for Computational Science, Institute for Molecular Science, 38 Nishigo-Naka, Myodaiji, Okazaki 444-8585, Japan

List of Tables

S1	Energies of the doublet and quartet spin states and the energy differences of the important stationary points along the LH and ER pathways.	3
S2	The reaction energy (E_{reaction}) and the barrier height ($E_{\text{activation}}$) for the gold-less oxidation of CO to CO ₂ calculated at all the levels of theory using 6-31+G* basis set. These values are compared with the experimentally reported NIST data.	3
S3	Absolute electronic energy values (in Hartrees) of all the intermediates involved in the reaction.	5

List of Figures

S1	Root mean square deviation (RMSD)/Å with respect to all the functionals for Int.1 (upper two) and Int.2 (lower two) via both ER and LH mechanisms.	4
S2	Different geometries obtained for Au ₃ -O on optimizing it using different DFT functionals.	5

Table S1: Energies of the doublet and quartet spin states and the energy differences of the important stationary points along the LH and ER pathways.

Complexes	E _{Doublet} (Hartree)	E _{Quartet} (Hartree)	Difference (kcal/mol)
ER Int.1	-520.4360912	-520.2853716	-94.58
ER T.S.	-670.5690663	-670.544833	-15.21
ER Int.2	-482.2699342	-482.2294996	-25.37
LH Int.1	-670.6233453	-670.5816781	-26.15
LH T.S.	-670.5848718	-670.5211016	-40.02
LH Int.2	-670.6787896	-670.6112357	-42.39

Energies of the quartet states were calculated using the PBE0 method based on the optimized geometries of the doublet states.

Table S2: The reaction energy (E_{reaction}) and the barrier height (E_{activation}) for the goldless oxidation of CO to CO₂ calculated at all the levels of theory using 6-31+G* basis set. These values are compared with the experimentally reported NIST data.

Functional	E _{reaction} (kcal/mol)	E _{activation} (kcal/mol)
NIST data	-7.8	—
CCSD(T)	-7.1	60.6
B2PLYP-D	-9.3	57.3
ω B97x-D	-8.7	61.4
cam-B3LYP	-7.5	62.8
lc-BLYP	-5.0	68.9
lc- ω PBE	-6.7	68.0
O3LYP	-6.4	55.7
X3LYP	-8.6	56.5
HSE1PBE	-12.1	56.5
MPW1K	-12.2	57.9
B3PW91	-10.3	55.3
B3P86	-9.3	52.8
BHandHLYP	-18.1	75.1
PBE0	-11.5	57.0
BP86	-2.3	—
PBE	-3.0	36.6
BLYP	-1.4	43.6
M06-L	-16.5	49.6
TPSSh	-11.0	51.0
VSXC	-7.7	54.2

Using Hess law and enthalpy of formation at 0 K from NIST data, enthalpy of goldless reaction: $\text{CO} + \text{O}_2 \rightarrow \text{CO}_2 + [\text{O}]$ is the difference of the enthalpy of formation of products and reactants, i.e., $=(-393.1+246.8)-(-113.8+0.0) = -32.5 \text{ kJ/mol} \sim -7.8 \text{ kcal/mol}$.

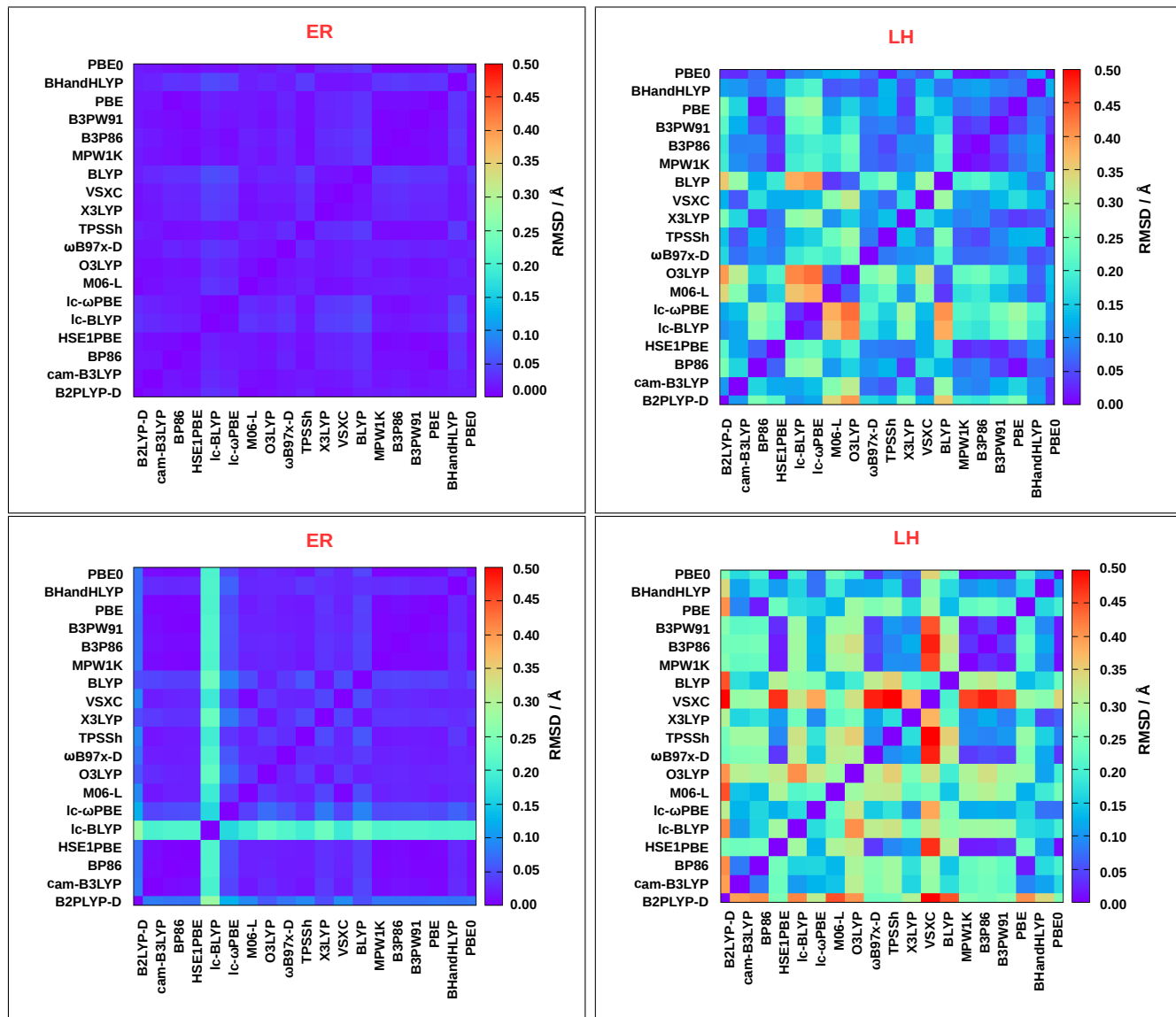


Figure S1: Root mean square deviation (RMSD)/Å with respect to all the functionals for Int.1 (upper two) and Int.2 (lower two) via both ER and LH mechanisms.

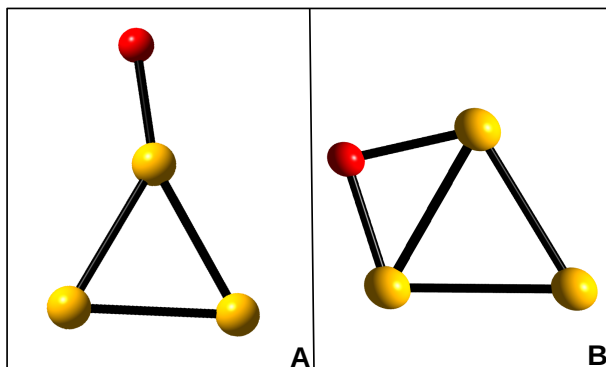


Figure S2: Different geometries obtained for $\text{Au}_3\text{-O}$ on optimizing it using different DFT functionals.

Table S3: Absolute electronic energy values (in Hartrees) of all the intermediates involved in the reaction.

Functional	Uncomplexed Reactants			ER				LH		
	Au_3	CO	O_2	Int1	T.S.	Int2	CO_2	Int1	T.S.	Int2
CCSD(T)	-404.854024	-113.045637	-149.9698704	-517.944137	-667.866123	-479.8394025	-188.124129	-667.928161	-667.881061	-667.98059768
B2PLYP-D	-406.3676837	-113.2244915	-150.207979	-519.640275	-669.803847	-481.4705256	-188.4367903	-669.8599429	-669.8186439	-669.9091178
ω B97x-D	-407.3847158	-113.2772846	-150.2772809	-520.7110916	-670.9436562	-482.5226926	-188.5269446	-671.001301	-670.9599207	-671.0530562
cam-B3LYP	-407.0599492	-113.2733199	-150.2820864	-520.3818662	-670.6180029	-482.201628	-188.5228294	-670.676503	-670.632845	-670.7310691
lc-BLYP	-406.5003067	-113.0596811	-150.0486128	-519.6163654	-669.62449	-481.5310328	-188.1950785	-669.6844557	-669.64753764	-669.7367868
lc- ω PBE	-407.2328029	-113.2377448	-150.2409456	-520.5244736	-670.719007	-482.3562354	-188.4682583	-670.7782555	-670.7151499	-670.8269254
O3LYP	-407.7197109	-113.2820634	-150.2888812	-521.0403058	-671.2836825	-482.8503136	-188.5369596	-671.337352	-671.2950333	-671.379766
X3LYP	-407.1854904	-113.2752901	-150.278709	-520.507084	-670.7462689	-482.316501	-188.5241703	-670.7992258	-670.7584648	-670.8462014
HSE1PBE	-407.1890641	-113.1982818	-150.1877397	-520.4418235	-670.5895864	-482.274463	-188.4071801	-670.6433423	-670.6046809	-670.6890666
MPW1K	-407.3916345	-113.2810415	-150.2867838	-520.7257068	-670.970213	-482.5266713	-188.5381727	-671.0246044	-670.9849222	-671.0711137
B3PW91	-407.4912033	-113.2663668	-150.2683576	-520.8101322	-671.0376585	-482.6161291	-188.5141646	-671.0914379	-671.0516885	-671.1348751
B3P86	-408.6762124	-113.5545291	-150.6021343	-522.2867729	-672.8531282	-483.9697112	-188.9715878	-672.9057815	-672.8685595	-672.9479507
BHandHLYP	-406.7939246	-113.2597819	-150.2513636	-520.0903712	-670.2890925	-481.9169772	-188.4913887	-670.3448535	-670.3220987	-670.4111245
PBE0	-407.340179	-113.1914025	-150.1743354	-520.4360912	-670.5690663	-482.2699342	-188.3899077	-670.6233453	-670.5848718	-670.6787896
BP86	-407.649568	-113.3149416	-150.337576	-521.0261788	-671.3419783	-482.825687	-188.5988213	-671.3894423	-671.3535953	-671.4266142
PBE	-407.1932425	-113.1878814	-150.1886804	-520.5952742	-670.7635344	-482.4411984	-188.4031968	-670.8101319	-670.775426	-670.8479266
BLYP	-407.1745601	-113.3036675	-150.3251372	-520.5277167	-670.828111	-482.3422829	-188.5749337	-670.8750751	-670.8367901	-670.9173049
M06-L	-407.4809367	-113.3015214	-150.3118331	-520.835649	-671.1255219	-482.6442809	-188.58159	-671.1723893	-671.1359907	-671.2318257
TPSSH	-407.0873448	-113.315368	-150.3283739	-520.4603312	-670.7593016	-482.2505935	-188.590844	-670.8105677	-670.7709796	-670.8477495
VSXC	-407.7915025	-113.3539642	-150.3692628	-521.1934062	-671.5372062	-482.9816933	-188.6502293	-671.5840956	-671.5482109	-671.6399523